Laser pump and synchrotron radiation probe microdiffraction for investigation of optical recording process

Shigeru Kimura[1], Nobuhiro Yasuda[1], Yoshimitsu Fukuyama[1], Kiminori Ito[2], Yoshihito Tanaka[2], Toshiyuki Matsunaga[3], Rie Kojima[4], Kazuya Hisada[4], Takashi Mihara[4], Akio Tsuchino[4], Norihito Fujinoki[3], Masahiro Birukawa[5], Masaki Takata[1,2] and Noboru Yamada[6]

[1] JASRI, 1-1-1 Kouto, Sayo-gun, Sayo-cho, Hyogo 679-5198, Japan, kimuras@spring8.or.jp, [2] RIKEN SPring-8 Center, 1-1-1 Kouto, Sayo-gun, Sayo-cho, Hyogo 679-5148, Japan, [3] R&D Division, Panasonic Corporation, 3-1-1 Yagumo-naka-machi, Moriguchi, Osaka 570-8501, Japan, [4] AVC Networks Company, Panasonic Corporation, 1-15 Matsuo, Kadoma, Osaka 571-8504, Japan, [5] On leave from Panasonic Corporation, [6] Kyoto University, Yoshida-honmachi, Sakyo-ku, Kyoto 606-8501, Japan

ABSTRACT

We have developed a system of laser-pump and synchrotron radiation probe microdiffraction to investigate the phase-change process on a nanosecond time scale of phase-change thin layers and/or nanometer-sized dots embedded in multi-layer structures,. The measurements were achieved by combining i) the pump-laser system with a pulse width of 300 ps, ii) a highly brilliant focused microbeam with wide peak-energy width ($\Delta E/E \sim 2\%$) made by focusing helical undulator radiation without monochromatization, and iii) a precise sample rotation stage to make repetitive measurements. We successfully detected a very weak time-resolved diffraction signal by using this system from 100-nm-thick $Ge_2Sb_2Te_5$ phase-change thin layers and $Ge_{10}Sb_{90}$ nanometer-sized dots embedded in the thermally managed multi-layered structure.

Key words: Phase Change, Synchrotron Radiation, Microdiffraction, $Ge_2Sb_2Te_5$, $Ge_{10}Sb_{90}$, Pump and Probe

1. INTRODUCTION

Digital versatile disks (DVDs) and Blu-ray Discs (BDs) are two of the most convenient storage devices for large amounts of information such as that in videos and digital photographs. These are due to extensive efforts and developments that have been made in the progress of device materials. The developed phase-change materials can reportedly complete the phase change process with 20-ns laser irradiation. However, faster phase changes are still required for next-generation optical recording media. To achieve this purpose, it is crucial to precisely observe the crystallization process on a nanosecond time scale.

We therefore developed a new system of laser-pump and SR probe microdiffraction [Fig. 1(a)] to investigate the phase-change processes in a real optical recording media structure.[1] We achieved this by combining i) a pump laser system with a pulse width of 300 ps and a repetition rate of 1 kHz, ii) a highly brilliant focused microbeam with peak-energy width ($\Delta E/E \sim 2\%$) accomplished by focusing helical undulator radiation without monochromatization, and iii) a precise sample disk rotation stage with a system of position feedback for repetitive measurements.

Using this system, we successfully revealed the laser-induced crystallization process in real time both for 100-nm-thick $Ge_2Sb_2Te_5$ phase-change thin layers[1] and $Ge_{10}Sb_{90}$ nanometer-sized dots[2] embedded in the thermally managed multi-layered structure.

2. INSTRUMENTATION

We improved the system of time-resolved microdiffraction we previously developed,[3,4] installed at the SPring-8 BL40XU helical undulator beamline. The system mainly consisted of a subsystem for laser-pump and SR probe measurements and a subsystem of x-ray microdiffraction with a sample rotation stage, as can be seen from the schematic in Fig. 1(a).

The previous system used a mode-locked Ti:sapphire laser oscillator equipped with a regenerative amplifier (Spectra-Physics, USA) that had a pulse width of 130 fs acting as a pump laser. However, $Ge_2Sb_2Te_5$ phase-change layers with

thicknesses of less than 200 nm were not crystallized by pump laser irradiation since the pulse width of 130 fs was too short to crystallize thin phase-change layers. We therefore enlarged the pulse width to 300 ps by omitting the pulse compression process from the system of femtosecond laser amplification. The modified laser system produced pulses with a pulse energy of 1 mJ, a wavelength of 800 nm, and a repetition rate of 948.98 Hz, which was 1/220 of the revolution frequency of the storage ring. The laser was synchronized to SR pulses to measure the change in time-dependent diffraction intensity due to the crystallization of the phase-change layers. Figure 1(b) to (d) show time charts of the laser and the SR pulses we used in the experiment. Detailed synchronization procedure was described in ref. 1. The probe SR pulses were detected by using an avalanche photodiode (APD) with a time resolution of 1.6 ns and stored in a multi-channel scaler (MCS). To accumulate repetitive data, we used the scattered pump laser pulses detected by using another APD as trigger pulses for the MCS.

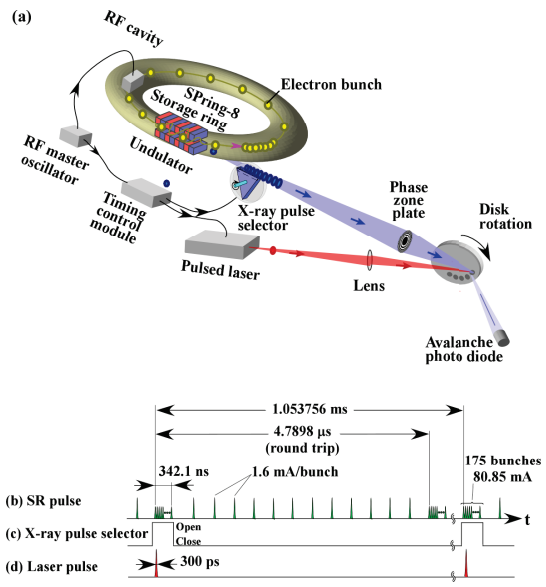

Fig. 1 Schematic of (a) set up for laser pump synchrotron radiation (SR) probe microdiffraction and time charts of (b) SR pulses, (c) gate of x-ray pulse selector, and (d) laser pulses.

A higher flux incident beam is required to detect very weak diffraction from the thin $Ge_2Sb_2Te_5$ phase-change layers embedded in a real device structure. We also need to simultaneously make many repetitive measurements for one sample disk to save the prepared sample volume. We adopted a wide energy width microbeam to satisfy both conditions created by focusing helical undulator radiation without monochromatization. A high-photon-flux beam ($\sim 10^{15}$ photons/s) can be used for quasi-monochromatic SR x-rays because the higher harmonics of the helical undulator are emitted toward an off-axial beam direction by extracting the central part of the radiation. The flux of the quasi-monochromatic SR x-rays is about 100 times that of monochromatized x-rays because of the peak energy width difference between that with (~0.02%) and that without (~2%) monochromatization. The quasi-monochromatic SR x-rays were focused on the disk sample by using a phase zone plate. We used a Ta phase zone plate with a diameter of 100 μm, an innermost zone radius of 5.0 μm, an outermost zone width of 250 nm, a zone number of 100, and a zone thickness of 2.5 μm, which was fabricated by NTT Advanced Technology Corporation, Japan.[5]

The quasi-monochromatic SR x-rays with a peak photon energy of 12 keV were pre-focused by two bend mirrors, whose focal point was located 8900 mm upstream of the phase zone plate. Only bunch train pulses then passed through the x-ray pulse selector (Jülich, Germany) with a repetition rate of 948.98 Hz, and they were focused on the sample position by using the phase zone plate [Fig. 1(a)]. The focal length of the zone plate was 240 mm. The horizontal and vertical beam sizes at the focal position (*i.e.*, the sample position) were 2.8 μm (vertically) × 3.5 μm (horizontally), which were determined by the knife edge scan method. The photon flux was 1.5×10^9 photons/s, even when only 0.38% of the SR x-rays passed through the x-ray pulse selector. We noted that the pulse selector also effectively prevented the zone plate from being destroyed due to radiation damage.

Diffraction was measured with a high precision diffractometer equipped with a sample disk rotation stage. The rotation stage maintained the overlap of the x-ray microbeam and the pump laser beam on the sample surface when the disk was rotating, which was achieved by using a low-eccentric spindle motor and a system of position feedback control.[1] This enabled us to use an x-ray microbeam for the repetitive measurements of x-ray diffraction.

3. CRYSTALLIZATION OF 100-nm-THICK $Ge_2Sb_2Te_5$ PHASE-CHANGE THIN LAYERS

We investigated the dependence of the crystallization process of a 100-nm-thick $Ge_2Sb_2Te_5$ thin layer embedded in a multilayered structure on laser power to demonstrate the capabilities of the system we developed. The layered structure of the disk sample is as follows. Both the top and bottom surfaces of the 100-nm-thick $Ge_2Sb_2Te_5$ layer were covered by 10-nm-thick ZnS (80 mol %)-SiO_2 (20 mol %) layers for passivation. A 40-nm-thick Ag layer was formed under the bottom ZnS-SiO_2 layer as a laser reflection layer, which is a typical layered structure in phase-change optical recording media. Commercial recording media generally have a polycarbonate (PC) substrate on the top ZnS-SiO_2 layer because the laser is irradiated through the PC substrate. However, we laid out an SiO_2 glass substrate (120 mm diameter and 1.1 mm thick) under the Ag layer to keep the surface flat when the disk was rotating. This is very

effective to keep the x-ray microbeam and the pump laser beam overlapping in the $Ge_2Sb_2Te_5$ layer even when using the feedback system. We believe this substrate change did not affect the phase-change process.

The sample disk was mounted on the rotation stage and the glancing angle for the x-ray beam was set to 12.0°. Because we confirmed that x-ray diffraction pattern of the $Ge_2Sb_2Te_5$ thin films showed NaCl type crystal structure as reported in ref. 6, the most intense 200 diffraction peak was detected with the APD, which was mounted on the 2θ-arm of the diffractometer and fixed to the diffraction angle of 19.5°.

Figure 2 shows the dependence of the time-resolved diffraction peak profiles on laser power due to the crystallization of the $Ge_2Sb_2Te_5$ layer in the sample disk with irradiation laser powers of (a) 476, (b) 420, (c) 355 and (d) 313 nJ. These were plotted by averaging the adjacent five channels of the MCS, meaning that the time resolution was 8 ns and the time zero was set to the time when the pump laser hits the sample disk. The measurement time was only 900 seconds (~ 9.0×10^5 shots) for each profile. All four profiles could be obtained with one sample disk. This is advantageous to investigate and compare the crystallization processes precisely by changing various conditions such as the irradiation laser power, wavelength, and pulse width.

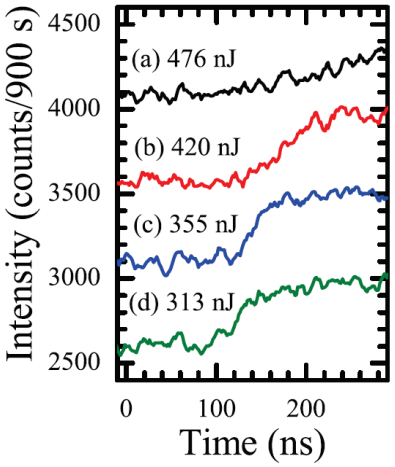

Fig. 2 Dependence of time-resolved diffraction peak profiles on laser power due to crystallization of 100 nm-thick $Ge_2Sb_2Te_5$ layer in sample disk with irradiation laser powers of (a) 476, (b) 420, (c) 355, and (d) 313 nJ. Note that profiles have been vertically displaced for clarity.

We observed distinct variations in the diffraction intensity profiles on a nanosecond time scale in this series of experiments as the irradiation laser power was changed from 313 to 476 nJ, as can be seen from Fig. 2. Except for (a), the diffraction intensity profiles begin to increase with a delay of approximately 100 to 120 ns after 300 ps laser irradiation. These are very similar to that of the previously measured 300-nm-thick $Ge_2Sb_2Te_5$ film.[1] On the other hand, the profile (a) shows a gradual increase of the intensity with shorter time delay. We think the laser power of 476 nJ causes the melt of the material film. This is the possible reason why the crystallization speed of (a) is slower than those of (b) to (d) which will be crystallized via solid process. Comparing (b) to (d), the time delay to start crystallization is a little different. As the laser power decreases from (b) to (d), the delay time becomes shorter. Because the crystallization process of the $Ge_2Sb_2Te_5$ is reported to be nucleation-dominant type,[7] we guess the delay time is the time for nucleation. This indicates precise control of the temperature profile due to laser irradiation is very important to realize faster phase-change.

4. CRYSTALLIZATION OF $Ge_{10}Sb_{90}$ NANOMETER-SIZED DOTS

Nanodot samples were formed with an amorphous $Ge_{10}Sb_{90}$ alloy with approximately 50-nm diameter.[2] These samples were fabricated by successive sputtering of multilayers on a patterned glass disk substrate with a diameter of 64- mm (HOYA Corp., Japan); on the glass substrate, UV-resin nanopillars with a diameter of 50- nm and a height of 100-nm were formed with a 100-nm pitch using the nano-imprinting technique.[8] The layer stack was designed to imitate the structure of a commercial phase-change optical disk; it was optically optimized to exhibit a large change in reflectivity corresponding to phase transition from the amorphous to crystalline state. It was also designed to suppress heat flow from $Ge_{10}Sb_{90}$ to the adjacent layers. According to previous reports, Sb-based phase-change alloys, including $Ge_{10}Sb_{90}$, were characterized by "growth-dominant crystallization" processes owing to their relatively low nucleation rates but high growth rates.[9] To overcome the low nucleation rates, we inserted pure Sb layers as seed layers to shorten the crystallization time because the Sb layer would be crystallized during or just after deposition and serve as a precursor for the $Ge_{10}Sb_{90}$ layer in each stack. A silver layer with thickness of 40-nm was provided to increase optical absorption in the $Ge_{10}Sb_{90}$ layer and also protect the resin pillars from thermal damages. The multilayers were deposited almost exclusively on the tops of the nanopillars to successfully form nanodot-recording elements. Approximately 2.4×10^{10} nanodots were formed in a zone (ϕ 33.0–35.4-mm) on a sample disk.

The size of the pump laser and probe SR beams on the sample surface were optimized according to the sample shape: approximately 10×100 μm^2 (laser) and 1.98×16.6 μm^2 (SR). Because the size of the x-ray beam was rather large, compared to that of the nanodots, we observed diffractions from approximately 1200 to 1300 nanodots within one shot. Moreover, because x-ray diffraction from one shot was very weak, we compiled cumulative diffraction data for every case by changing the position of the sample for every shot. Once we confirmed that the x-ray diffraction peaks

of the $Ge_{10}Sb_{90}$ nanodots used in this study exhibited rhombohedral symmetry *R-3m* resembling pure Sb,[10] we observed the change in the diffraction intensity of the 012 signal, the most intense peak of the rhombohedral structure.

Figure 3 shows the experimental results of time-resolved diffraction intensity of the 012 peak,. Each curve was obtained by accumulating data from approximately 100,000 shots and plotted by averaging the adjacent ten data, meaning that the time resolution was 16 ns, to smooth the curves. All diffraction intensity profiles begin to increase with a delay of approximately 70 to 100 ns and saturated at approximately 150 ns after 300 ps laser irradiation. Comparing (a) to (d), the time delay to start crystallization is a little different. As the laser power decreases from (a) to (d), the delay time becomes a shorter. This indicates that it may be effective to set the pumping laser power to slightly above the threshold of crystallization for minimizing the crystallization time.

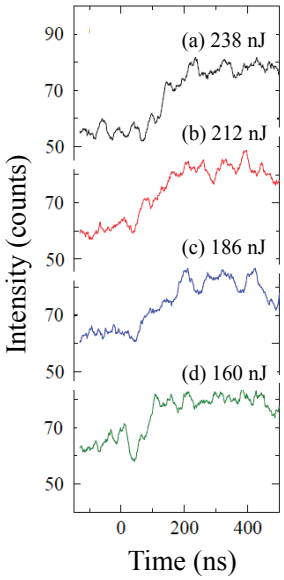

Fig. 3 Dependence of time-resolved diffraction intensity on laser power due to crystallization of the $Ge_{10}Sb_{90}$ nanodots with irradiation laser powers of (a) 238, (b) 212, (c) 186, and (d) 160 nJ.

5. CONCLUTION

We successfully revealed the laser-induced crystallization processes in real time for 100-nm-thick $Ge_2Sb_2Te_5$ phase-change thin layers and $Ge_{10}Sb_{90}$ nanometer-sized dots embedded in the thermally managed multi-layered structure using the system of laser-pump and SR probe microdiffraction we newly developed. The system will be a very effective tool for exploring the faster phase-change materials and device structures for the next generation.

ACKOWLEADGMENT

We are deeply grateful to Koji Sekiguchi, Kazuhiko Fujiie, and Osamu Kawakubo of Sony Corporation for their huge efforts in the preparation of the nanodot samples. SR experiments were carried out at BL40XU of SPring-8 (Proposal Nos. 2010A0030, 2010B0030, 2011A0030, 2011B0030, 2012A0030, and 2012B0030).

REFERENCES

[1] N. Yasuda, Y. Fukuyama, S. Kimura, K. Ito, Y. Tanaka, H. Osawa, T. Matsunaga, R. Kojima, K. Hisada, A. Tsuchino, M. Birukawa, N. Yamada, K. Sekiguchi, K. Fujiie, O. Kawakubo, and M. Takata, Rev. Sci. Instrum.**84**, 063902 (2013).

[2] N. Yamada, R. Kojima, K. Hisada, T. Mihara, A. Tsuchino, N. Fujinoki, M. Birukawa, T. Matsunaga, N. Yasuda, Y. Fukuyama, K. Ito, Y. Tanaka, S. Kimura, and M. Takata, Adv. Opt. Mat. **1**, (2013), in press.

[3] Y. Fukuyama, N. Yasuda, J. Kim, H. Murayama, Y. Tanaka, S. Kimura, K. Kato, S. Kohara, Y. Moritomo, T. Matsunaga, R. Kojima, N. Yamada, H. Tanaka, T. Ohshima, and M. Takata, Appl. Phys. Express **1**, 045001 (2008) .

[4] Y. Tanaka, Y. Fukuyama, N. Yasuda, J. E. Kim, H. Maruyama, S. Kohara, H. Osawa, T. Nakagawa, S. Kimura, K. Kato, F. Yoshida, H. Kamioka, Y. Moritomo, T. Matsunaga, R. Kojima, N. Yamada, H. Tanaka, K. Toriumi, T. Ohshima, H. Tanaka, and M. Takata, Jpn. J. Appl. Phys. **48**, 03A001 (2009).

[5] N. Yasuda, H. Murayama, Y. Fukuyama, J. Kim, S. Kimura, K. Toriumi, Y. Tanaka, Y. Moritomo, Y. Kuroiwa, K. Kato, H. Tanaka, M. Takata, J. Synchrotron Rad. **16**, 352 (2009).

[6] N. Yamada and T. Matsunaga, J. Appl. Phys. **88**, 7020 (2000).

[7] T. Matsunaga, J. Akola, S. Kohara, T. Honma, K. Kobayashi, E. Ikenaga, R. O. Jones, N. Yamada, M. Takata, and R. Kojima, Nature Mat. **10**, 129 (2011).

[8] K. Suzuki, H. Kobayashi, T. Sato, H. Yamashita, T. Watanabe, Proc. SPIE **8166**, 81663B (2011).

[9] L. van Pieterson, M. H. R. Lankhorst, M. van Schijndel, A. E. T. Kuiper, J. H. J. Roosen, J. Appl. Phys. **97**, 083520 (2005)..

[10] P. Zalden, C. Bichara, J. van Eijk, C. Braun, W. Bensch, M. Wuttig, J. Appl. Phys. **107**, 104312 (2010).